Determination of breakdown voltage of $In_{0.53}Ga_{0.47}As$/InP single photon avalanche diodes

Peng Zhou (周 鹏)[1], Changjun Liao (廖常俊)[2], Zhengjun Wei (魏政军)[2], Chunfei Li (李淳飞)[1*], and Shuqiong Yuan (袁书琼)[2]

[1]*Department of Physics, Harbin Institute of Technology, Harbin 150001, China*

[2]*Lab of Photonic Information Technology, School for Information and Optoelectronic Science and Engineering, South China Normal University, Guangzhou 510631, China*

[*]*Corresponding author: cfli@hit.edu.cn*

Received June 5, 2010; accepted August 20, 2010; posted online January 1, 2011

We examine the saturation of relative current gain of $In_{0.53}Ga_{0.47}As$/InP single photon avalanche diodes (SPADs) operated in Geiger mode. The punch-through voltage and breakdown voltage of the SPADs can be measured using a simple and accurate method. The analysis method is temperature-independent and can be applied to most SPADs.

OCIS codes: 040.1345, 040.3060, 040.5160, 040.5570.
doi: 10.3788/COL201109.010402.

Some avalanche photodiodes (APDs) that are reverse biased beyond breakdown voltage and are operated in Geiger mode may achieve single photon detection[1−10]. These APDs are also known as Geiger mode avalanche photodiodes or single photon avalanche diodes (SPADs)[2]. Breakdown voltage V_B, an important parameter for APDs applied in both linear mode and Geiger mode, is theoretically defined as the voltage threshold above which the gain is infinite. When experimentally determining the breakdown voltage, other approximate definitions are used, typically defining V_B as the reverse bias voltage 1) when the dark current I_{dark} reaches 100 μA[3,4]; 2) when the multiplication factor (or mean gain) G_m reaches 100[5]; and 3) when the output pulses exceed 100 mV (0.5 mV at the device)[6]. These definitions are good approximations but will meet their limitations when the APD is used as a SPAD. SPADs require that V_B be more accurately determined. When adopting Definition 1, the critical value of the dark current should be revalued for different SPADs at different temperatures. Current-voltage (I-V) characteristics vary significantly for different SPADs. Moreover, the dark current decreases with temperature when it reaches the breakdown value I_B. With Definition 2, G_m is difficult to measure accurately near breakdown, especially for thin structures, because G_m further increases with the voltage in such structures[7]. This definition will lead to underestimation of the breakdown voltage. The output of the SPADs is affected by many factors, including material, device structure, and operating conditions. Therefore, if the amplitude of the output pulse is monitored as the evidence of breakdown in Definition 3, the critical value also has to be revalued. In this letter, we demonstrate that the breakdown voltage can be correctly determined by analyzing the I-V curves which have been extended to a voltage higher than its breakdown value by using a passive quench circuit.

The avalanche breakdown of a SPAD, which can be initiated by both photocarriers and dark carriers, is a complicated process, but can be simplified to a few steps[11]. The SPAD is reverse biased above V_B. An initial carrier (or electron-hole pair) triggers the impact ionization. The density of the free carriers rises swiftly around the injected point. The avalanche then increasingly spreads by transverse diffusion of the free carriers (in shallow junctions)[11] or by reabsorption of the photons emitted from hot carrier relaxations (in reach-through structures)[12]. The avalanche current rises accordingly until it reaches the value at which the quenching occurs.

For an explication of the analysis above, we built an extensively adopted I-V characterizing system, using a passive quench circuit. A schematic diagram of the experimental setup and its equivalent circuit are shown in Fig. 1. The device investigated was an 80-μm-diameter separate absorption charge multiplication (SACM) $In_{0.53}Ga_{0.47}As$/InP APD of type C30645 from EG&G, which was proven suitable for use as a SPAD. The total dark current was 10 nA when G_m was 10 at a temperature of 300 K. It was dry-air-sealed in a chamber cooled down by Peltier effect. The avalanche current quenched itself by developing a voltage drop on a ballast resistor of 200 kΩ. The mean current was measured by an amperemeter. V_{DC} is the bias supply voltage, R_L is the quenching resistance, R_d is the diode impedance which is the series of ohmic resistance and space charge

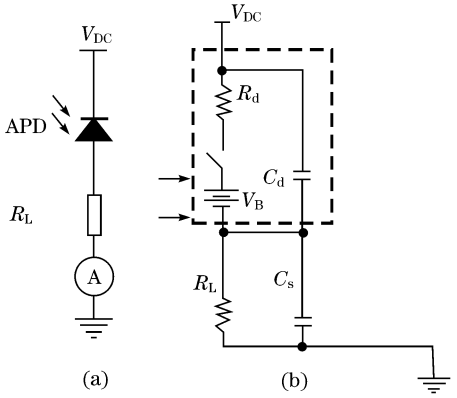

Fig. 1. (a) Schematic diagram of the experimental setup and (b) its equivalent circuit.

resistance, $C_{\rm d}$ and $C_{\rm s}$ are the diode capacitance and the capacitance of anode to ground, respectively. The value of $R_{\rm d}$ is around 1 kΩ.

The triggering of the avalanche corresponds to closing the switch in the equivalent circuit, as shown in Fig. 1(b). During the quenching, the transient voltage on the diode $V_{\rm d}(t)$ is given as

$$V_{\rm d}(t) = \frac{R_{\rm L}}{R_{\rm d}+R_{\rm L}}(V_{\rm DC}-V_{\rm B})\exp\left(-\frac{t}{RC}\right) + \frac{R_{\rm d}R_{\rm L}}{R_{\rm d}+R_{\rm L}}\left(\frac{V_{\rm DC}}{R_{\rm L}}+\frac{V_{\rm B}}{R_{\rm d}}\right), \quad (1)$$

where R is $R_{\rm d}$ and $R_{\rm L}$ in parallel, and C is the sum of $C_{\rm d}$ and $C_{\rm s}$:

$$R = \frac{R_{\rm d}R_{\rm L}}{R_{\rm d}+R_{\rm L}}, \quad (2)$$

$$C = C_{\rm d}+C_{\rm s}. \quad (3)$$

$V_{\rm d}(t)$ exponentially falls toward the steady-state value of $V_{\rm f}$:

$$V_{\rm f} = \frac{R_{\rm d}R_{\rm L}}{R_{\rm d}+R_{\rm L}}\left(\frac{V_{\rm DC}}{R_{\rm L}}+\frac{V_{\rm B}}{R_{\rm d}}\right) = V_{\rm B}+R_{\rm d}I_{\rm f}, \quad (4)$$

where

$$I_{\rm f} = \frac{V_{\rm DC}-V_{\rm B}}{R_{\rm d}+R_{\rm L}} \quad (5)$$

is the steady state value of the current. The deduced formulas of Eqs. (4) and (5) are consistent with those in other references[13].

A measured curve similar to the curves published in one of our resluts[5], including punch-through and breakdown, is shown in Fig. 2. The output of a pigtailed distributed feedback (DFB) diode laser of 1550-nm wavelength was attenuated to −45 dBm and used as input signal. The device was cooled down to −25 °C during measurement. As shown in Fig. 2, the photocurrent $I_{\rm p}$ starts to increase at $V_{\rm DC}=25$ V, while the dark current-voltage curve still remains unchanged near this voltage.

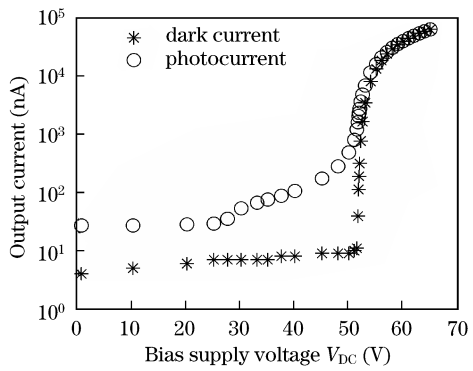

Fig. 2. I-V curve for dark current and photocurrent of the 80-μm-diameter $In_{0.53}Ga_{0.47}As$/InP APD at temperature of −25 °C.

$I_{\rm p}$ as well as the dark current $I_{\rm d}$ increases sharply at the voltage near 50 V, and the slope reduces when $V_{\rm DC}$ exceeds 51.8 V. The punch-through voltage for this APD is 30 V, but this cannot be indicated clearly in the figure.

To learn more about the data from the experiment, we plotted the relative current gain $G_{\rm r}$ which is defined as

$$G_{\rm r} = 1 + R_{\rm L}\frac{{\rm d}I_{\rm o}}{{\rm d}V} \quad (6)$$

versus $V_{\rm DC}$ in Fig. 3, where $I_{\rm o}$ is the output current (dark current or photocurrent). The constant 1 is arbitrarily chosen just to avoid zero in the logarithmic plot. As shown in the figure, there is a sudden jump of $G_{\rm r}$ for $I_{\rm p}$ from 1 at a voltage of 30 V, clearly indicating the punch-through. At the voltage above the punch-through value, photocarriers created within the absorption layer can be swept into the multiplication layer by the nonzero electric field. $G_{\rm r}$ for $I_{\rm d}$ is approximately 1 when $V_{\rm DC}$ is below 50 V, as well as $G_{\rm r}$ for $I_{\rm p}$ before punch-through. $G_{\rm r}=1$ means that there is no avalanche multiplication. $G_{\rm r}$ begins to saturate and no longer rises with $V_{\rm DC}$ when it reaches 51.8 V. In this letter, $V_{\rm B}$ is defined as the voltage when $G_{\rm r}$ is saturated at a constant other than 1. Therefore, $V_{\rm B}$ is 51.8 V for the APD used in the experiment at −25 °C.

The next step of our investigation is to explain the saturation effect and the definition of $V_{\rm B}$. The current measured by the amperemeter is neither the instantaneous current nor the steady-state current, but the ensemble average value. It is equal to the total charge of the response pulse accumulated in unit time.

Avalanche quenching corresponds to opening the switch in the equivalent circuit of Fig. 1(b). The voltage of the device APD can be easily obtained from the differential equation for the equivalent circuit and can be

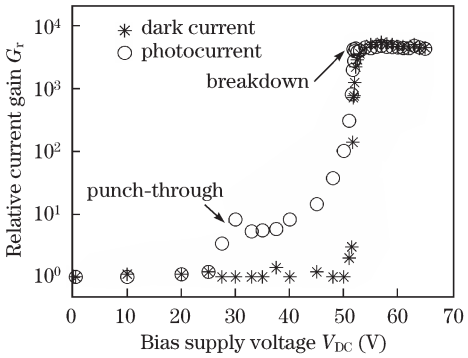

Fig. 3. Relative current gain as a function of the voltage on the APD clearly shows the punch-through and breakdown voltage.

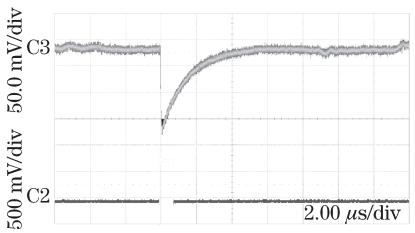

Fig. 4. Waveform of avalanche.

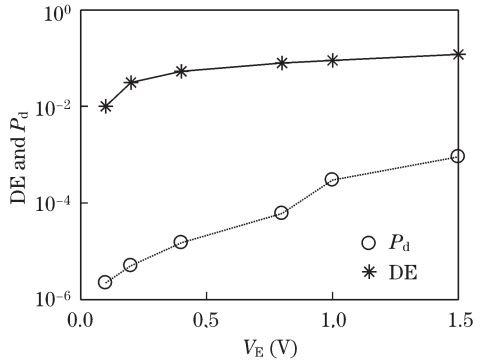

Fig. 5. Dark count probability P_d and detection efficiency (DE) versus excess voltage V_E.

represented as

$$V_d(t) = V_{DC} + (V_B - V_{DC}) \exp\left(-\frac{t}{T_R}\right), \quad (7)$$

where T_R is one of the characteristic time constants of the circuit and is given as

$$T_R = (C_d + C_s) R_L. \quad (8)$$

V_d recovers above V_B and may trigger another avalanche breakdown during the recovery. The charge of the avalanche pulse Q_p is

$$Q_p = (V_d - V_B)(C_d + C_s). \quad (9)$$

In the measurement, the power of the incident light is relatively high compared with the photon counting level. At voltages above V_B, the probability for a single carrier to trigger the breakdown, which is the function of the excess voltage V_E, rises from zero to a unit[14,15] with V_E. Therefore, detection efficiency asymptotically leans toward a certain value as the excess voltage rises. For a large amount of photons, the breakdown will occur continuously. Therefore, V_d will recover to a voltage lower than a reference voltage V_r but with a fluctuation not as low as that of V_{DC}. The value of V_r depends on the distribution of single photon breakdown probability versus excess voltage. The output current I_o can be represented as

$$\begin{aligned} I_o &= (V_r - V_B)(C_d + C_s) N \\ &= I_f \frac{T_R}{t_r}\left[1 - \exp\left(-\frac{t_r}{T_R}\right)\right], \end{aligned} \quad (10)$$

where N is the average avalanche rate in unit time, and t_r is the time needed for V_d to recover to V_r from V_B. In our experiment, $t_r = 0.2858 T_R$, resulting in an I_o value of $0.8698 I_f$. The value of V_r predicted by Eqs. (7) and (10) agrees with that monitored by the oscilloscope. Both t_r and T_R are independent of V_{DC}, but I_f is a linear function of V_{DC}, therefore I_o has a linear dependence on V_{DC}. G_r is saturated at a voltage above breakdown according to Eq. (10).

The waveform of the avalanche is shown in Fig. 4. A direct current (DC) voltage of 51.7 V superposing the 0.8-V gate voltage is applied on the APD. The excess voltage is 0.7 V, corresponding to I_f of about 3.5 μA, while the measured I_o is 4.1 μA. As shown in the figure, t_r is about 0.1 μs, while T_R is 0.4 μs. Both V_r (51.9 V and alternating current (AC) portion about 160 mV) and I_o agree with the values predicted by Eqs. (7) and (10).

In Fig. 5, the dark count probability per gate and the detection efficiency are plotted as functions of the excess voltage. Gate pulses of 5 ns full-width at half-maximum (FWHM) are applied to the APD after combining with a DC bias of 51.3 V at a temperature of 228 K.

In conclusion, we examine the saturation of the relative current gain. The punch-through voltage and breakdown voltage of SPADs can be measured using a simple and accurate method. The analysis used in this letter is temperature-independent and can be applied to most SPADs.

This work was supported by the National Basic Research Program (973 Program) of China (Nos. G2001039302 and 007CB307001) and the Guangdong Key Technologies R&D Program (No. 2007B010400009).

References

1. Z. Wei, K. Li, P. Zhou, J. Wang, C. Liao, J. Guo, R. Liang, and S. Liu, Chin. Phys. B **17,** 4142 (2008).
2. J. S. Ng, C. H. Tan, and J. P. R. David, J. Mod. Opt. **51,** 1315 (2004).
3. T. Maruyama, F. Narusawa, M. Kudo, M. Tanaka, Y. Saito, and A. Nomura, Opt. Eng. **41,** 395 (2002).
4. C. Y. Park, K. S. Hyun, S. G. Kang, and H. M. Kim, Appl. Phys. Lett. **67,** 3789 (1995).
5. J. G. Rarity, T. E. Wall, K. D. Ridley, P. C. M. Owens, and P. R. Tapster, Appl. Opt. **39,** 6746 (2000).
6. Y. S. Hyun and C. Y. Park, J. Appl. Phys. **81,** 974 (1996).
7. M. M. Hayat, Ü. Sakoğu, O. Kwon, S. Wang, J. C. Campbell, B. E. A. Saleh, and M. C. Teich, IEEE J. Quantum Electron. **39,** 179 (2003).
8. L. Yin, Q. Chen, and G. Gu, Acta Opt. Sin. (in Chinese) **29,** (s2) 283 (2009).
9. F. Zhao, B. Zhao, X. Zhang, W. Li, W. Zou, X. Sai, and Y. Wei, Acta Opt. Sin. (in Chinese) **29,** 3236 (2009).
10. F. Yang, Y. He, T. Zhou, and W. Chen, Acta Opt. Sin. (in Chinese) **29,** 21 (2009).
11. A. Lacaita, A. Spinelli, and S. Longhi, Appl. Phys. Lett. **67,** 2627 (1995).
12. A. Lacaita, S. Cova, A. Spinelli, and F. Zappa, Appl. Phys. Lett. **62,** 606 (1992).
13. S. Cova, M. Ghioni, A. Lacaita, C. Samori, and F. Zappa, Appl. Opt. **35,** 1956 (1996).
14. S. Wang, F. Ma, X. Li, G. Karve, X. Zheng, and J. C. Campbell, Appl. Phys. Lett. **82,** 1971 (2003).
15. D. A. Ramirez, M. M. Hayat, G. Karve, J. C. Campbell, S. N. Torres, B. E. A. Saleh, and M. C. Teich, IEEE J. Quantum Electron. **42,** 137 (2006).